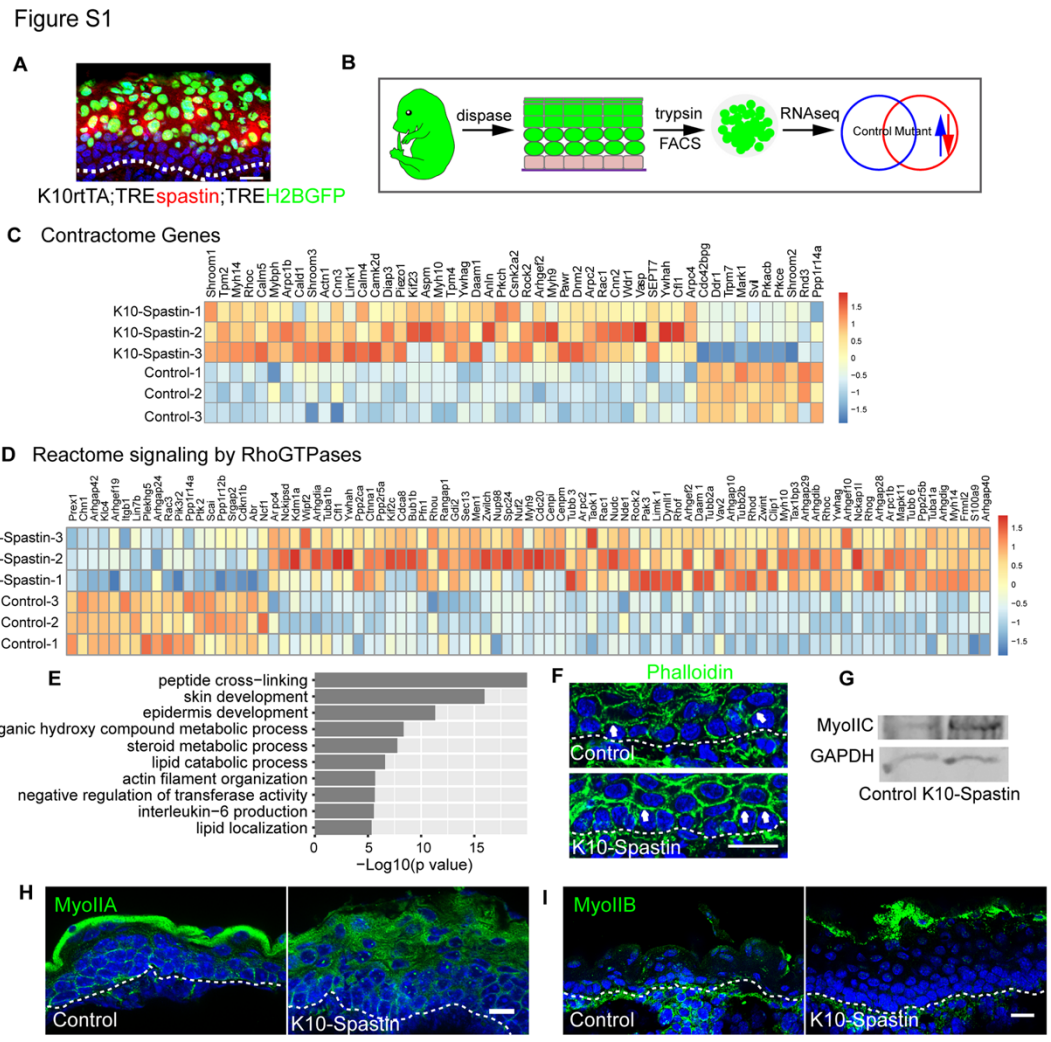

Figure S1. Microtubule disruption increases cortical actomyosin. Related to Figure 1.

(A) Immunostaining of HA labeled spastin (red) in K10rtTA;TREspastin;TRE-H2B-GFP, showing co-expression of spastin with H2B-GFP in suprabasal cells at E16.5. Scale bar, 20 μm.
(B) Diagram of RNA-Seq sample preparation. Only H2B-GFP labeled Krt10+ suprabasal cells from control and K10-Spastin were sorted for RNA isolation. n= 3 embryos for each group.
(C) RNA-Seq heatmap depicting differential expression of contractome genes in K10-Spastin and control suprabasal cells. Gene expression by FPKM is centered and $\log_2$-transformed.
(D) RNA-Seq heatmap depicting differential expression of the Rho-GTPase reactome signaling genes in K10-Spastin and control suprabasal cells. Gene expression by FPKM is centered and $\log_2$-transformed.
(E) Gene Ontology (GO) term enrichment analysis of genes (fold-change>2, $p<0.01$, FDR<0.05) for K10-Spastin compared to control, revealing upregulation of skin development and actin filament organization related biology process upon microtubule disruption.
(F) Increased F-actin (phalloidin in green) at the interface between basal and spinous cells in control and K10-Spastin epidermis. Arrows indicate the interface between basal and suprabasal cells. Scale bar, 20 μm.
(G) Western blot of Myosin IIC and GAPDH in K10-Spastin and control epidermis at E16.5.
(H) Immunostaining of Myosin IIA in K10-Spastin and control epidermis at E16.5. Scale bar, 20 μm.
(I) Immunostaining of Myosin IIB in K10-Spastin and control epidermis at E16.5. Scale bar, 20 μm.

Figure S2

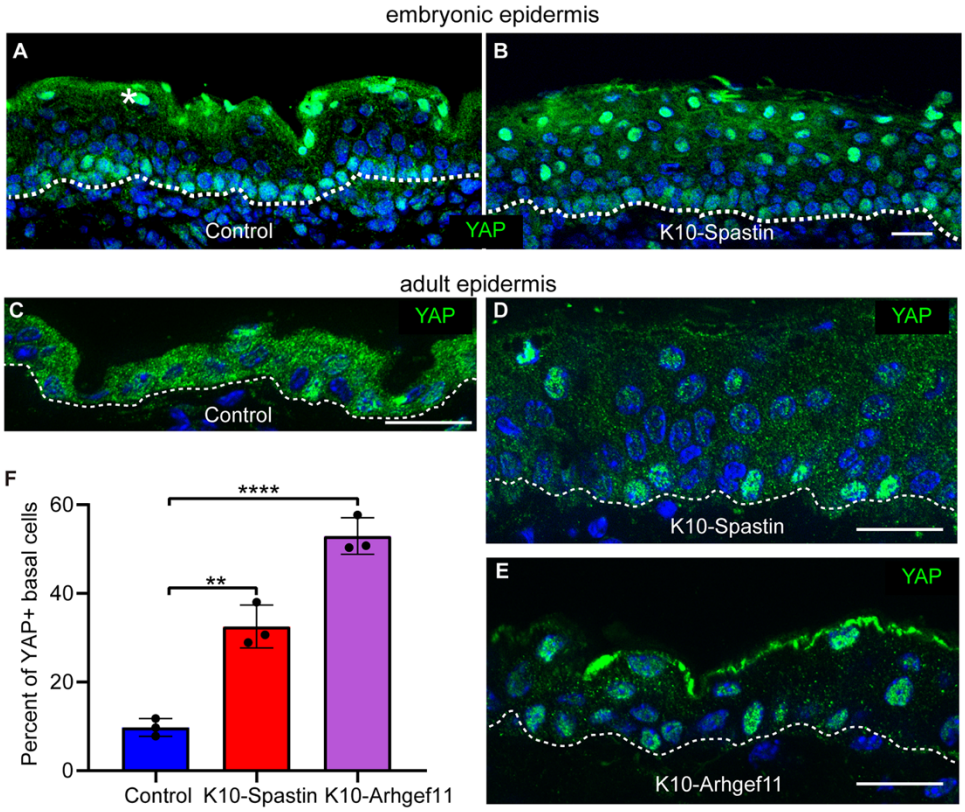

Figure S2. Microtubule depolymerization increases nuclear YAP in the epidermis. Related to Figure 2.

(A and B) Immunofluorescence staining of YAP (green) in control and K10-Spastin epidermis. This antibody showed non-specific labeling in the periderm. Notice the increased nuclear YAP signaling in the suprabasal cells in K10-Spastin. Scale bar, 20 μm.
(C-E) Immunostaining of YAP (green) in P33 adult skin epidermis from control (C), K10-Spastin [(D), doxycycline for two weeks] and K10-Arhgef11 [(E), doxycycline for 1 day] mice.
(F) Quantification of the percent of YAP positive basal cells in control, K10-Spastin and K10-Arhgef11 epidermis. Data are shown as the mean +/- SD. n=3 mice for control (27 fields), K10-Spastin (28 fields) and K10-Arhgef11 (14 fields) were measured, p-value<0.01 for control to K10-Spastin, p-value<0.0001 for control to K10-Arhgef11, two-tailed unpaired t-test.

Figure S3

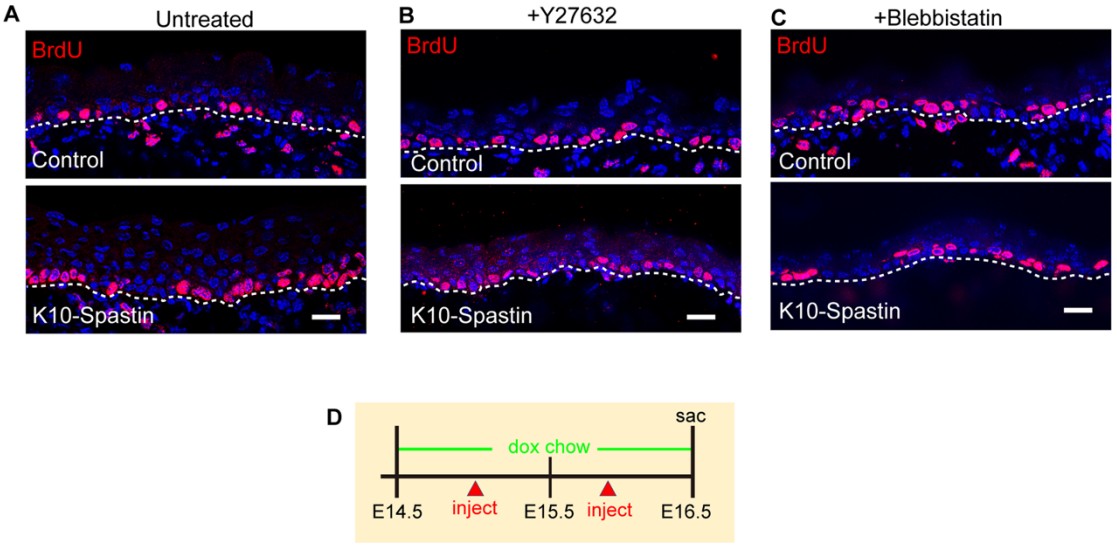

Figure S3. Inhibiting contractility rescues the basal cell hyperproliferation caused by microtubule depolymerization. Related to Figure 3.

(A-C) Immunofluorescence staining of BrdU in the untreated (A), Y27632 (B), and blebbistatin (C) injected control (top) and K10-Spastin (bottom) epidermis. Scale bars, 20 μm.
(D) Diagram depicting the drug injection times in K10-Spastin. Pregnant dams were fed with doxycycline chow from E14.5, injected with inhibitors twice (one early in the morning and one at night) the next day, and injected with BrdU 1 hour before sacrifice at E16.5.

Figure S4

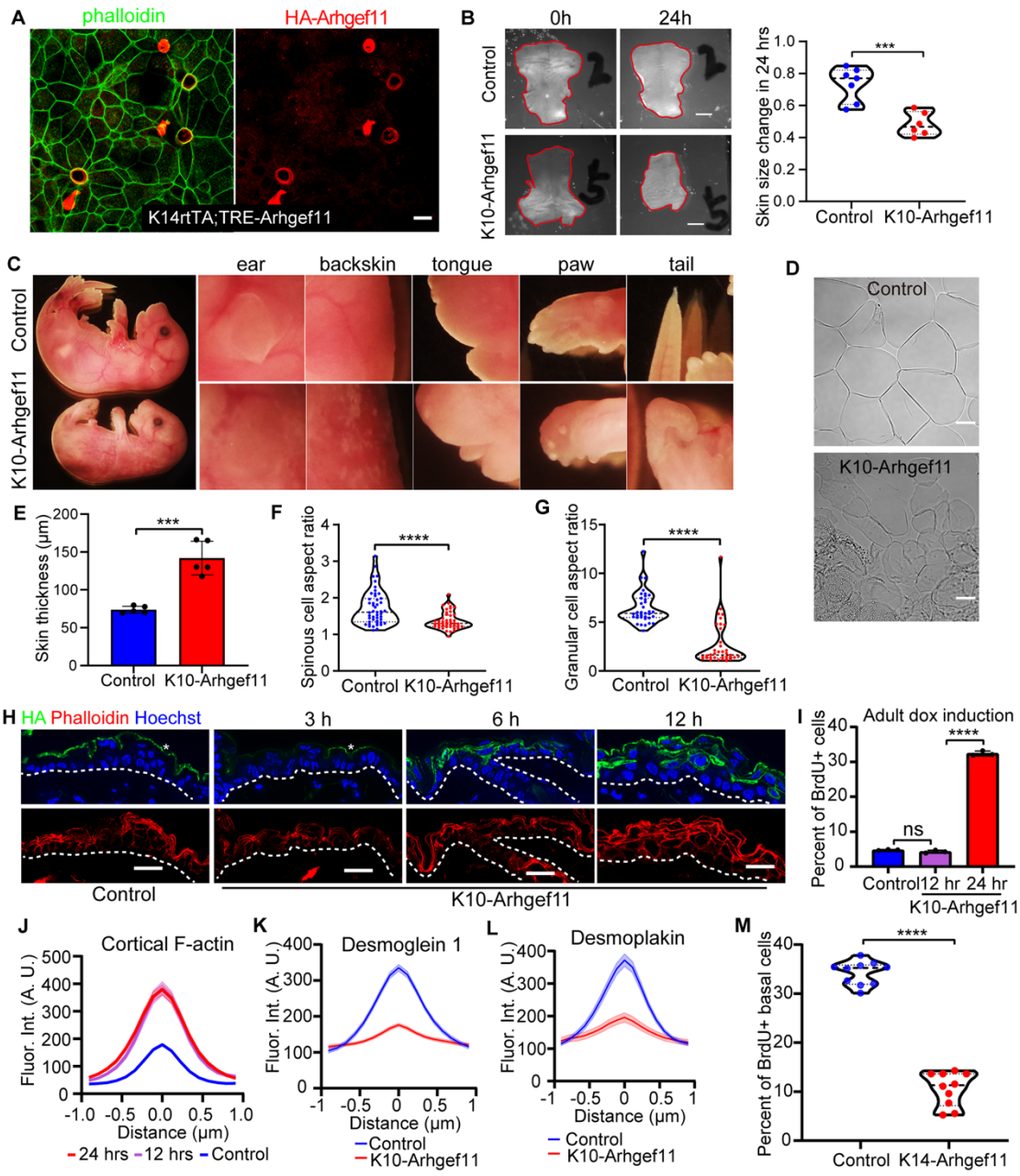

Figure S4. Increasing contractility by expressing Arhgef11^{CA} in differentiated cells induces skin thickening and cell rounding. Related to Figure 4.

(A) Immunostaining of F-actin (phalloidin, green) and HA-Arhgef11 (red) in keratinocytes transduced with K14-rtTA and pTRE2-Arhgef11 plasmids. These cells were treated with doxycycline and also with calcium to induce junction formation. Scale bar, 20 μm.

(B) Skin explants from control and K10-Arhgef11 embryos at the beginning (E15.5) and 24 hours later (sustained with 2 μg/ml doxycycline). Scale bar, 1mm. Changes in skin explant area over 24 hours are shown at right. n=7 embryos for control and n=6 for K10-Arhgef11 from 3 litters were measured, p-value<0.001, two-

tailed unpaired t-test.
(C) Arhgef11^{CA} expression in differentiated cells of the epidermis leads to thick flaky skin, lack of external ears, misshapen paws, exposed tongues, and curly tails.
(D) Isolated corneocytes from control and K10-Arhgef11 neonates at P0. Notice the abnormal morphology in K10-Arhgef11. Scale bars, 20 μm.
(E) Quantification of skin thickness in K10-Arhgef11 and control at E17.5. Data are shown as the mean ± SD, n=5 embryos for control (489 regions) and K10-Arhgef11 (304 regions), p-value<0.001, two-tailed unpaired t-test.
(F and G) Quantification of spinous (F) and granular (G) cell aspect ratio in K10-Arhgef11 and control. For spinous cell quantification, n=3 embryos for control (47 cells) and K10-Arhgef11 (44 cells). For granular cells quantification, n=3 embryos for control (35 cells) and K10-Arhgef11 (36 cells. p-value<0.0001, two-tailed unpaired t-test.
(H) Immunofluorescence staining of HA-Arhgef11 and F-actin in control (left) and K10-Arhgef11 (after 3 hrs, 6 hrs and 12 hrs of doxycycline treatment) adult (P67) epidermis. Asterisks indicate non-specific HA staining in corneocytes. Scale bars, 20 μm.
(I) Percentage of BrdU+ basal cells at different time point upon doxycycline treatment in control and K10-Arhgef11 epidermis. Data shown as the mean ± SD, n=3 mice for control (24 fields), 12 hrs (25 fields) and 24 hrs (23 fields) of K10-Arhgef11, for control to 12 hrs, p-value=0.1260, for 12 hrs to 24 hrs, p-value<0.0001, two-tailed unpaired t-test.
(J) Quantification of fluorescence intensity of cortical F-actin at different time points after doxycycline administration. Data shown as the mean ± SEM, n=32 cells for control, and n=49 cells for 12 hours, and n=48 cells for 24 hours of K10-Arhgef11 from 3 embryos. For 12 hrs to control, p-value<0.0001, 24 hrs to control, p-value<0.0001, p=0.89 for 12 hrs to 24 hrs, two-tailed unpaired t-test.
(K) Measurement of desmoglein 1 intensity in differentiated cell of K10-Arhgef11 and control E17.5 backskin. Data shown as the mean ± SEM, n=48 cells for control and n=50 cells for K10-Arhgef11 from 3 embryos, p-value <0.0001, two-tailed unpaired t-test.
(L) Measurement of desmoplakin intensity in differentiated cells of K10-Arhgef11 and control E17.5 backskin. Data shown as the mean ± SEM, n=40 cells for control and n=43 cells for K10-Arhgef11 from 3 embryos, p-value <0.0001, two-tailed unpaired t-test.
(M) Quantification of BrdU+ basal cells in control and K14rtTA; TREArhgef11 (K14-Arhgef11) at E16.5. Only HA+ basal cells from K14-Arhgef11 were analyzed for their proliferation. n=10 fields from 2 embryos for control (742 cells) and K14-Arhgef11 (266 HA+ cells) were quantified. Data are shown as the mean ± SD, p-value<0.0001, two-tailed unpaired t-test.

Figure S5

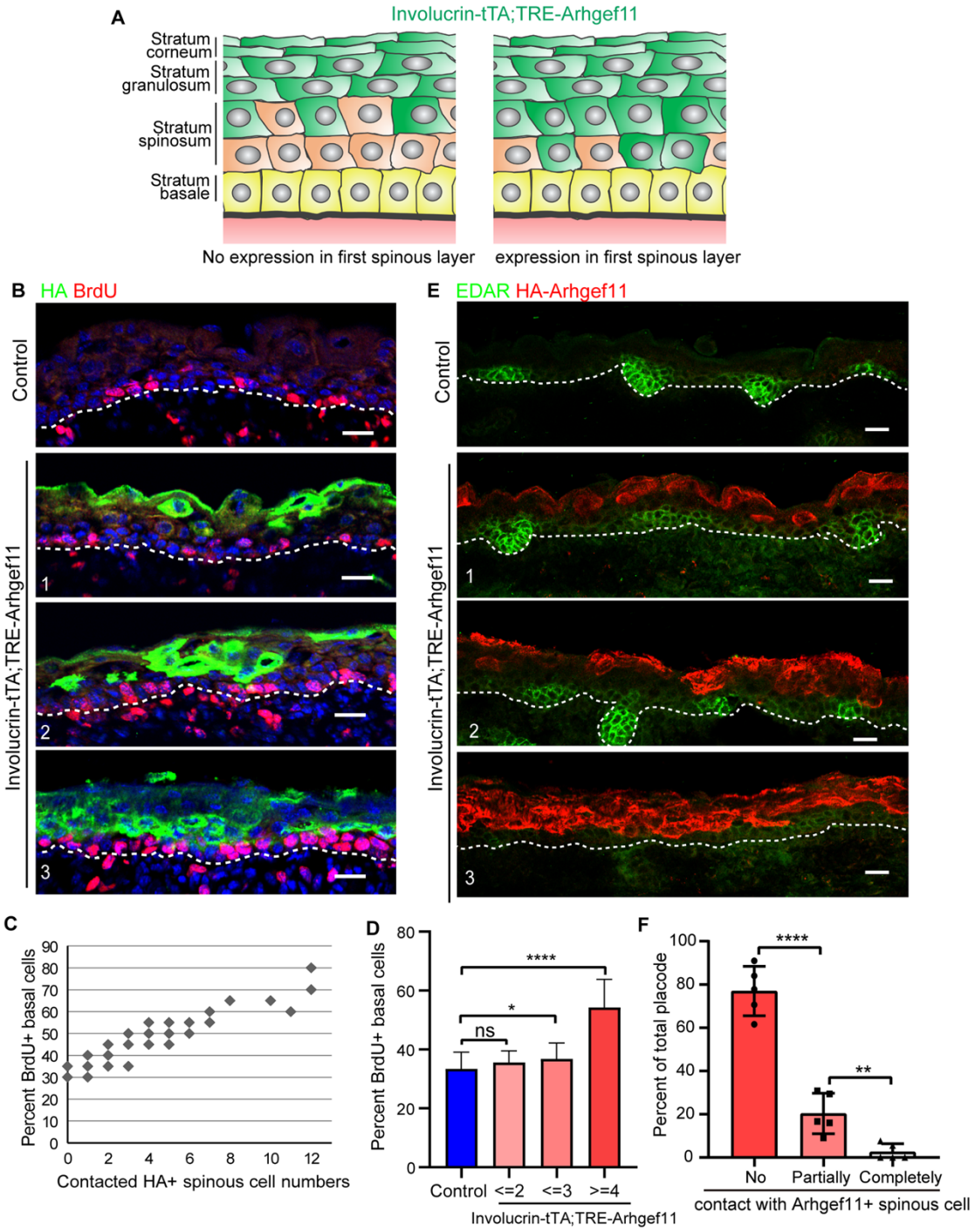

Figure S5. Increased contractility of cells not directly in contact with stem cells does not cause increased proliferation. Related to Figure 4.

(A) Diagram depicting mosaic expression in the epidermis of Involucrin-tTA;TRE-Arhgef11. In most regions, at E16.5, the expression is as shown on the left. However, in some focal areas, there is expression in immediate spinous cells as shown on the right.

(B) BrdU (red) and HA (green) immunofluorescence staining in Involucrin-tTA;TRE-Arhgef11 and control at

E16.5, doxycycline chow was removed at E12.5 to induce expression. Images 1, 2, 3 show different effects on basal cell proliferation relating to contact variations with HA-Arhgef11^{+ve} spinous cells. Scale bars, 20 μm.
(C) Quantification of BrdU+ basal cells in control and Involucrin-tTA;TRE-Arhgef11. We quantitated random regions of epidermis that spanned 20 basal cells. In these regions, the number of BrdU+ and basal cell-contacted HA+ spinous cells were quantified. Notice that the percent of BrdU+ cells is significantly increased when there were over 3 contacted spinous cells expressing Arhgef11^{CA}. n=34 regions for control from 3 embryos and n=52 regions from 4 embryos. For analysis of control to (contacted HA+ spinous <=2), p-value= 0.1001, not significant; control to (contacted HA+ spinous<=3), p-value= 0.0172 (<0.05, significant); control to (contacted HA+ spinous>=4), p-value <0.0001. Data are shown as the mean ± SD, two-tailed unpaired t-test.
(D) Quantitation of BrdU+ basal cells, binned according to the numbers of contacting spinous cells expressing Arhgef11^{CA}.
(E) Placode marker EDAR (green) and HA (red) immunofluorescence staining in control and Involucrin-tTA;TRE-Arhgef11. Scale bar, 20 μm. Images 1, 2, 3 shows different effects on placode formation relating to contact variations with HA-Arhgef11+ spinous cells.
(F) Percent of placodes in Involucrin-tTA; TRE-Arhgef11 embryos based on contact with Arhgef11^{CA} spinous cells or not ('no' means 0, 'partially' means >=1 cells, completely means placode fully covered with Arhgef11^{CA} cells). Data shown as the mean ± SD, n=5 mutants (97 placodes) were analyzed. For the analysis: no contact to partially contact: p-value<0.0001; partially to completely contact: p-value<0.01. Two-tailed unpaired t-test.
All mice for A-F were at E16.5, doxycycline chow was removed at E12.5 to induce expression.

Figure S6

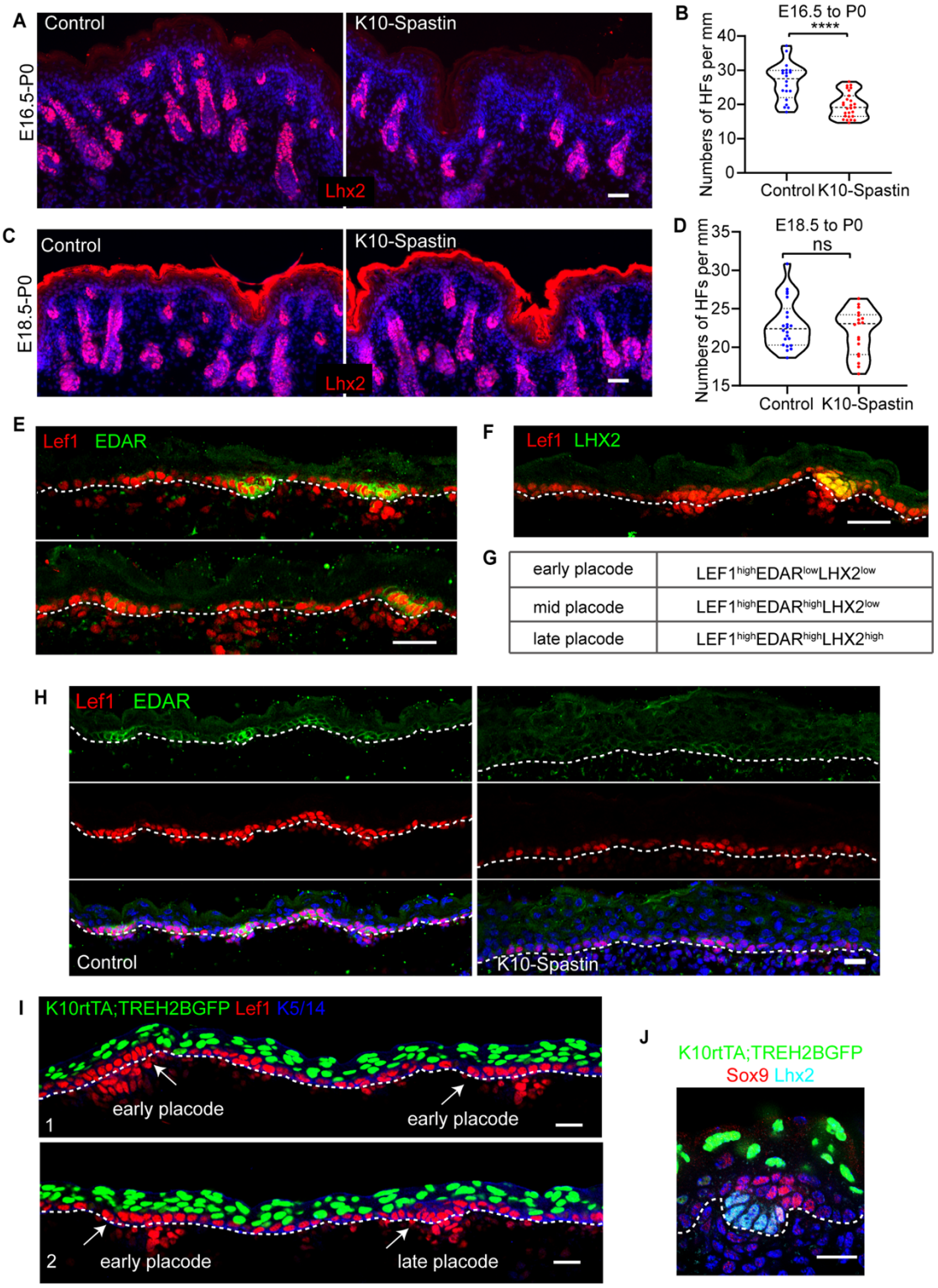

Figure S6. Increasing contractility in differentiated cells causes non-cell autonomous defects in hair follicle specification. Related to Figure 5 and Figure 6.

(A and B) Staining of Lhx2 (red) in P0 control and K10-Spastin (doxycycline treatment began at E16.5) epidermis. Notice the normal development of the HFs that are already specified. Scale bar, 50 μm. n=20 fields for control and n=27 fields for K10-Spastin from 2 embryos were measured, p-value<0.0001, two-tailed unpaired t-test.
(C and D) Staining of Lhx2 (red) in P0 control and K10-Spastin skin (doxycycline treatment began at E18.5). Scale bar, 50 μm. n=22 fields for control and n=18 fields for K10-Spastin from 2 embryos were measured, p-value= 0.3023, not significant, two-tailed unpaired t-test.
(E) Staining of Lef1 (red) and EDAR (green) in control skin at E16.5. Notice the $LEF1^{high}$ but $EDAR^{low}$ early placode. Lef1 labels both the placode and dermal condensates below them. Scale bar, 30 μm.
(F) Staining of Lef1 (red) and Lhx2 (green) in control skin at E16.5. Notice the $Lef1^{high}$ but $Lhx2^{low}$ early placode; Lhx2 labels only late stage placodes. Scale bar, 30 μm.
(G) Criteria for labeling placodes as early, mid and late.
(H) Co-staining of EDAR and Lef1 in control and K10-Spastin skin at E16.5, related to Figures 6F-6G. Scale bar, 20 μm.
(I) Staining of Lef1 (red) and Krt5/14 (blue, basal layer marker) in K10-rtTA;TRE-H2B-GFP skin at E16.5. Note that there are no H2B-GFP labeled cells in either the early (image 1) or late placode (image 2). Scale bars, 20 μm.
(J) Staining of Sox9 (red) and Lhx2 (cyan) in K10-rtTA;TRE-H2B-GFP skin at E16.5, showing no H2B-GFP induction in Sox9+ suprabasal cells in the late placode. Scale bar, 20 μm.

Figure S7

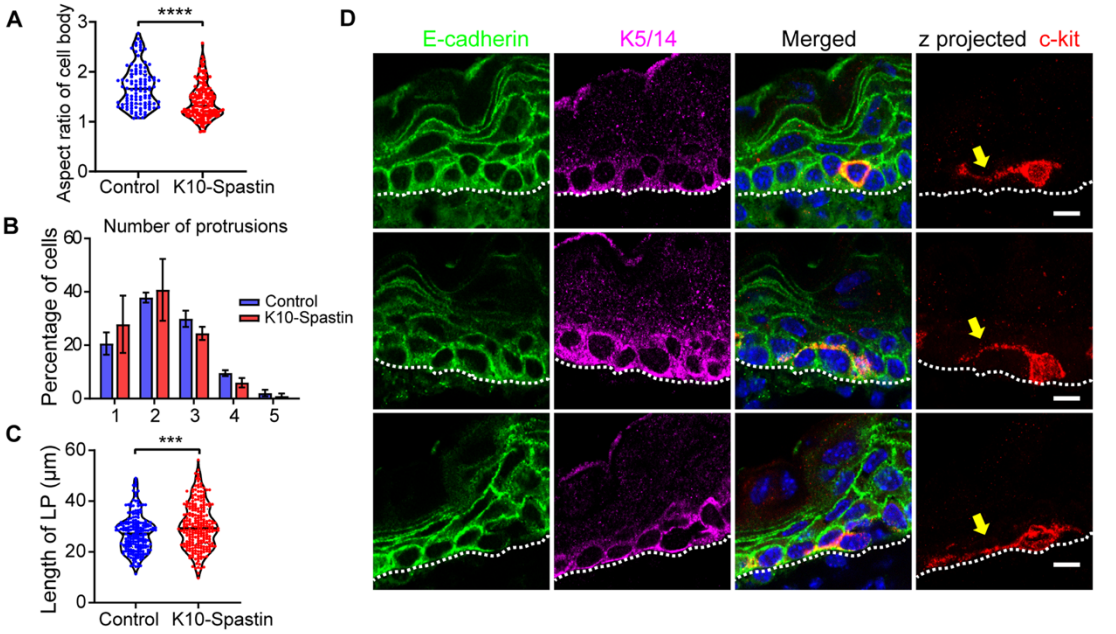

E Model

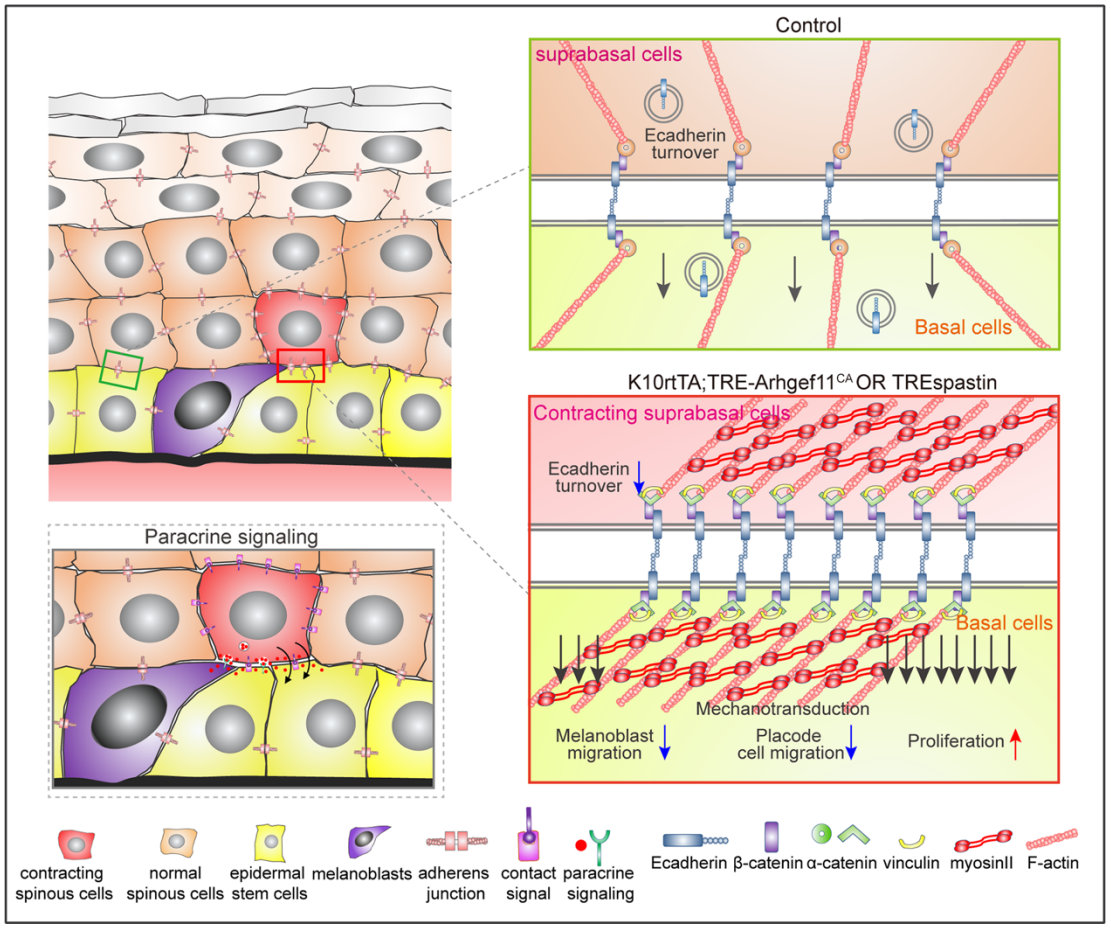

Figure S7. Increasing contractility in differentiated cells decreases migration of melanoblasts. Related to Figure 7.

(A) Quantification of the aspect ratio of melanoblast cell bodies in control and K10-Spastin epidermis. n=110 melanoblasts for control and n=156 melanoblasts for K10-Spastin from 3 embryos, p-value<0.0001, two-tailed unpaired t-test.
(B) Quantification of melanoblast protrusion numbers in control and K10-Spastin. Data shown as the mean ± SD, n=3 embryos for control (320 melanoblasts) and for K10-Spastin (311 melanoblasts), p-value>0.9999, not significant, two-tailed paired t-test.
(C) Lengths of the melanoblast leading protrusion (LP) in control and K10-Spastin epidermis. n=205 melanoblasts for control and n=237 melanoblasts for K10-Spastin from 3 embryos, p-value<0.001, two-tailed unpaired t-test.
(D) Co-staining of E-cadherin (green), the melanoblast marker C-kit (red) and the basal cell marker (Krt5/14) in control epidermis at E16.5. Arrows indicate the protrusions. Notice melanoblasts form protrusions that traverse through lateral junctions, above the basement membrane, and at the interface between suprabasal and basal cells. Scale bar, 10 μm.
(E) Model of regulation of basal stem cell proliferation and migration by their differentiated progeny. Our data demonstrate that differentiated suprabasal cells form part of the niche that controls the behavior of the underlying stem cells. Under normal conditions, basal stem cells are adhered to suprabasal spinous cells through adherens junction (and other structures) that are under low tension and rapid turnover. Increased contractility results in increased proliferation and decreased migration of underlying cells. There are two general models to explain this. First (lower left), contractility of daughter cells could alter their cell surface compositions or their secretomes, allowing them to signal to basal cells in a paracrine manner. A second possibility, which is not mutually exclusive, is that mechanical coupling through adherens junctions drives these phenotypes. In this case, either the increased stability of adherens junctions, or the increased tension across them would be the signal that inhibits migration and/or promotes proliferation.